



A “seabird-eye” on mercury stable isotopes and cycling in the Southern Ocean

Marina Renedo^{a,b,*}, Paco Bustamante^{a,c}, Yves Cherel^d, Zoyne Pedrero^b, Emmanuel Tessier^b, David Amouroux^{b,**}

^a Littoral Environnement et Sociétés (LIENSs), UMR 7266 CNRS-La Rochelle Université, 2 rue Olympe de Gouges, 17000 La Rochelle, France

^b Université de Pau et des Pays de l'Adour, E2S UPPA, CNRS, IPREM, Institut des Sciences Analytiques et de Physico-chimie pour l'Environnement et les Matériaux, Pau, France

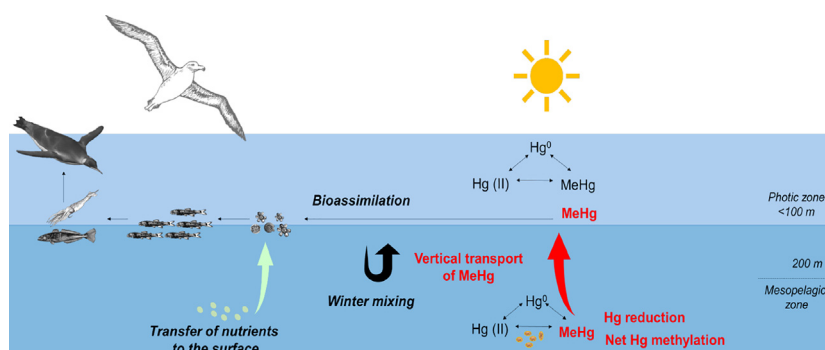
^c Institut Universitaire de France (IUF), 1 rue Descartes, 75005 Paris, France

^d Centre d'Etudes Biologiques de Chizé (CEBC), UMR 7372 CNRS-La Rochelle Université, 79360 Villiers-en-Bois, France

HIGHLIGHTS

- We assessed blood Hg isotopes in Antarctic, Subantarctic and Subtropical seabirds.
- Similar MeHg photodemethylation extent was estimated at distant latitudes.
- Most of the MeHg accumulated in seabirds seems to have a mesopelagic origin.
- Higher biogenic transformations of Hg potentially occur in subtropical waters.
- Regional mixed layer depth dynamics highly contribute to MeHg vertical transport.

GRAPHICAL ABSTRACT



ARTICLE INFO

Article history:

Received 3 April 2020

Received in revised form 22 June 2020

Accepted 23 June 2020

Available online 27 June 2020

Editor: Mae Sexauer Gustin

Keywords:

Methylmercury
Biogeochemistry
Latitude
Penguins
Skuas

ABSTRACT

Since mercury (Hg) biogeochemistry in the Southern Ocean is minimally documented, we investigated Hg stable isotopes in the blood of seabirds breeding at different latitudes in the Antarctic, Subantarctic and Subtropical zones. Hg isotopic composition was determined in adult penguins (5 species) and skua chicks (2 species) from Adélie Land (66°39'S, Antarctic) to Crozet (46°25'S, Subantarctic) and Amsterdam Island (37°47'S, Subtropical). Mass-dependent (MDF, $\delta^{202}\text{Hg}$) and mass-independent (MIF, $\Delta^{199}\text{Hg}$) Hg isotopic values separated populations geographically. Antarctic seabirds exhibited lower $\delta^{202}\text{Hg}$ values (-0.02 to 0.79 ‰, min-max) than Subantarctic (0.88 to 2.12 ‰) and Subtropical (1.44 to 2.37 ‰) seabirds. In contrast, $\Delta^{199}\text{Hg}$ values varied slightly from Antarctic (1.31 to 1.73 ‰) to Subtropical (1.69 to 2.04 ‰) waters. The extent of methylmercury (MeHg) photodemethylation extrapolated from $\Delta^{199}\text{Hg}$ values was not significantly different between locations, implying that most of the bioaccumulated MeHg was of mesopelagic origin. The larger increase of MDF between the three latitudes co-varies with MeHg concentrations. This supports an increasing effect of specific biogenic Hg pathways from Antarctic to Subtropical waters, such as Hg biological transformations and accumulations. This “biogenic effect” among different productive southern oceanic regions can also be related to different mixed layer depth dynamics and biological productivity turnover that specifically influence the vertical transport between the mesopelagic and the photic zones. This study shows the first Hg isotopic data of the Southern Ocean at large scale and reveals how regional Southern Ocean dynamics and productivity control marine MeHg biogeochemistry and the exposure of seabirds to Hg contamination.

© 2020 Elsevier B.V. All rights reserved.

* Correspondence to: M. Renedo, Littoral Environnement et Sociétés (LIENSs), UMR 7266 CNRS-La Rochelle Université, 2 rue Olympe de Gouges, 17000 La Rochelle, France.

** Corresponding author.

E-mail addresses: marina.renedo@ird.fr (M. Renedo), david.amouroux@univ-pau.fr (D. Amouroux).

1. Introduction

Although the Southern Ocean is usually perceived as a pristine area untouched by anthropogenic pressures, contaminants can nonetheless reach this region by ocean circulation and atmospheric transport (Fitzgerald et al., 2007). Mercury (Hg) is considered a globally distributed contaminant of major concern for humans and wildlife, especially in its methylmercury (MeHg) form (Eagles-Smith et al., 2018). Indeed, MeHg is a potent organometallic neurotoxin that accumulates in living organisms and that biomagnifies within food webs (Mason et al., 1996; Watras et al., 1998). The Hg biogeochemical cycle is highly complex and comprises several chemical processes and biological transformations, such as methylation/demethylation and redox reactions, that control MeHg production and its bioavailability to marine organisms. Hg methylation is thought to be mainly driven by anaerobic microorganisms within the water column down to at least the oxygen minimum zone (Lehnherr et al., 2011; Heimbürger et al., 2015). Due to biomagnification processes, top predators are exposed to high levels of MeHg, thereby presenting severe health risks for their populations (Tartu et al., 2013; Goutte et al., 2014a, 2014b).

In the Southern Ocean, particularly in the Indian Ocean sector, various studies have reported significant levels of Hg bioaccumulation in top predators such as seabirds (Carravieri et al., 2014, 2017, 2020; Cherel et al., 2018), with a common MeHg concentration trend exhibiting 4 to 8-fold higher concentrations in Subtropical relative to Antarctic populations for all of the seabird species studied to date (Carravieri et al., 2014, 2017). There is however a paucity of information in regard to Hg concentrations, spatial distribution, and speciation in the water column from this remote area of the world's oceans (Cossa et al., 2011; Lamborg et al., 2014; Canário et al., 2017). Complex oceanic dynamics along the Southern Ocean regions induce changes in the properties and subduction/upwelling rates of water masses (Sallée et al., 2010), thereby influencing the vertical advection of MeHg in the water column (Cossa et al., 2011), and consequently its availability for its assimilation within the marine food web. Substantial inter-seasonal variations also result in build-up of Hg-enriched surface waters during winter months and its subsequent downward transfer during spring and early summer (Cossa et al., 2011) before the shallow mixed layer is re-established (Sallée et al., 2010).

The study of Cossa et al. (2011) is the only one to date investigating latitudinal variations of methylated Hg (MeHg and dimethylmercury (Me₂Hg)) and the distribution in the water column of the Southern Ocean. This study revealed slightly higher concentrations in Antarctic seawaters (0.15 to 0.21 pmol L⁻¹) compared to Subantarctic and Subtropical seawaters (0.08 to 0.10 pmol L⁻¹). Although these data only reflected a single seasonal setting, this north to south gradient of increasing MeHg concentrations in water is opposite to the trend observed in the tissues of seabirds (Becker et al., 2016; Carravieri et al., 2014, 2017, 2020; Cherel et al., 2018). However, the seasonal mismatch (March–April) between the sampling campaign of Cossa et al. (2011) and studies during seabird breeding stages (November–February) (Carravieri et al., 2014, 2017, 2020) must be carefully considered because intra-annual fluctuations in vertical oceanic dynamics, atmospheric deposition, primary productivity, and light irradiance availability could affect MeHg production, transformations and transport in the water column. The spatial range of methylated Hg concentrations (MeHg and Me₂Hg) reported in the Southern Ocean water column might drive variations in biota MeHg concentrations. However, seasonal and geographical differences in Hg atmospheric deposition and Hg release during the melting of sea-ice can greatly influence Hg concentrations in the water column. Therefore, Hg assimilation efficiency for primary producers might also be altered, thereby making this association much more complex. For instance, higher productivity in Antarctic and Polar Front zones (Sullivan et al., 1993; Sokolov, 2008), could dilute biologically the MeHg, then reducing its uptake at the base of the food web (Pickhardt et al., 2002). Additionally, differences in food web

complexities between ecosystems (Cherel et al., 2007; Bost et al., 2009), could induce a differential MeHg biomagnification, leading to different levels of exposure in top predators (Lavoie et al., 2013).

The measurement of subtle deviations in naturally occurring Hg stable isotope ratios provides a new and powerful perspective for the exploration of the cycle of this element, and it has been shown to be useful to depict Hg sources or to quantify its reactivity within different environmental compartments (Blum et al., 2014). Hg has seven isotopes that experience mass-dependent and mass-independent isotopic fractionation (MDF and MIF, respectively). Most biogeochemical processes such as volatilization, reduction, absorption, demethylation, and methylation induce MDF (usually reported as $\delta^{202}\text{Hg}$) (Kritee et al., 2007, 2009; Rodriguez Gonzalez et al., 2009; Zheng and Hintelmann, 2010). Aqueous photochemical processes (MeHg photodemethylation and inorganic Hg photoreduction) have been shown to lead to significant levels of MIF of odd Hg isotopes ($\Delta^{199}\text{Hg}$ and $\Delta^{201}\text{Hg}$) (Bergquist and Blum, 2007; Zheng and Hintelmann, 2009; Perrot et al., 2012). Intracellular odd-MIF was recently discovered during photomicrobial MeHg demethylation and Hg(II) reduction in a marine microalga in the presence or absence of UV-B light (Kritee et al., 2017). MIF of even-mass Hg isotopes, reported as $\Delta^{200}\text{Hg}$ and $\Delta^{204}\text{Hg}$ (i.e., anomalous fractionation of the $^{200/198}\text{Hg}$ and $^{204/198}\text{Hg}$ ratio from the theoretical MDF line), was first detected in rainfall samples and is thought to be associated to mechanisms occurring in the atmosphere, such as photo-oxidation in the upper tropopause and/or neutron capture in space (Gratz et al., 2010; Chen et al., 2012; Cai and Chen, 2015). This signature is increasingly being investigated as a potential tracer of Hg sources of atmospheric origin. Consequently, the combination of Hg MDF and MIF signatures provide interesting and complementary information for potential sources and transformation pathways of Hg. In the Southern Ocean, Hg isotopic investigations in sediments and biota are limited to the Antarctic sector (Zheng et al., 2015; Liu et al., 2019), and as a result, the information about the biogeochemical cycle of Hg in larger zones across Antarctic remote oceanic regions remains insufficient (Bowman et al., 2020).

Seabirds are meso- to top- predators that forage in various compartments of the pelagic ecosystems. Several studies have demonstrated the usefulness of seabirds to assess Hg contamination as far as the biological characteristics are mastered (e.g. moulting patterns, migration or foraging strategies) (Furness and Camphuysen, 1997; Carravieri et al., 2013, 2016; Bustamante et al., 2016). Chicks of flying birds and both chick and adult penguins (a group of diving birds) are the most pertinent seabird models for tracing local Hg contamination pathways using Hg isotopic approaches because they reflect the Hg contamination around the colony (Blévin et al., 2013; Renedo et al., 2018a). Previous studies extensively explored the physiological, ecological and environmental aspects concerning the specific application of skua chicks and adult penguins for effective biomonitoring of Hg contamination at a large scale of the Southern Ocean (Carravieri et al., 2016, 2017). Therefore, the use of skua chicks and adult penguins for Hg isotopic investigations provides significant advantages in regard to the survey of Hg sources and its associated biogeochemical processes in the ocean (Point et al., 2011; Day et al., 2012; Zheng et al., 2015; Renedo et al., 2018b). Moreover, non-lethal sampling of feathers (reflecting the inter-moult period) and blood (reflecting short-term exposure) provides complementary and specific spatio-temporal information of Hg exposure in adults (Renedo et al., 2018a). Since blood Hg reflects recent Hg acquisition over the last weeks preceding sampling (Bearhop et al., 2000), the Hg isotopic composition of blood of chicks and penguins is considered as indicative of local exposure with a relevant resolution (Renedo et al., 2018a). In this work, we investigated the Hg isotopic composition (mainly as MeHg; Renedo et al., 2018a) of blood cells of two seabird models (skua chicks and adult penguins) in Antarctic, Subantarctic and Subtropical zones (Fig. 1). We hypothesized that the specific regional MeHg dynamics and transfer to the marine pelagic trophic chain at different latitudes of the Southern Indian Ocean could lead to significant

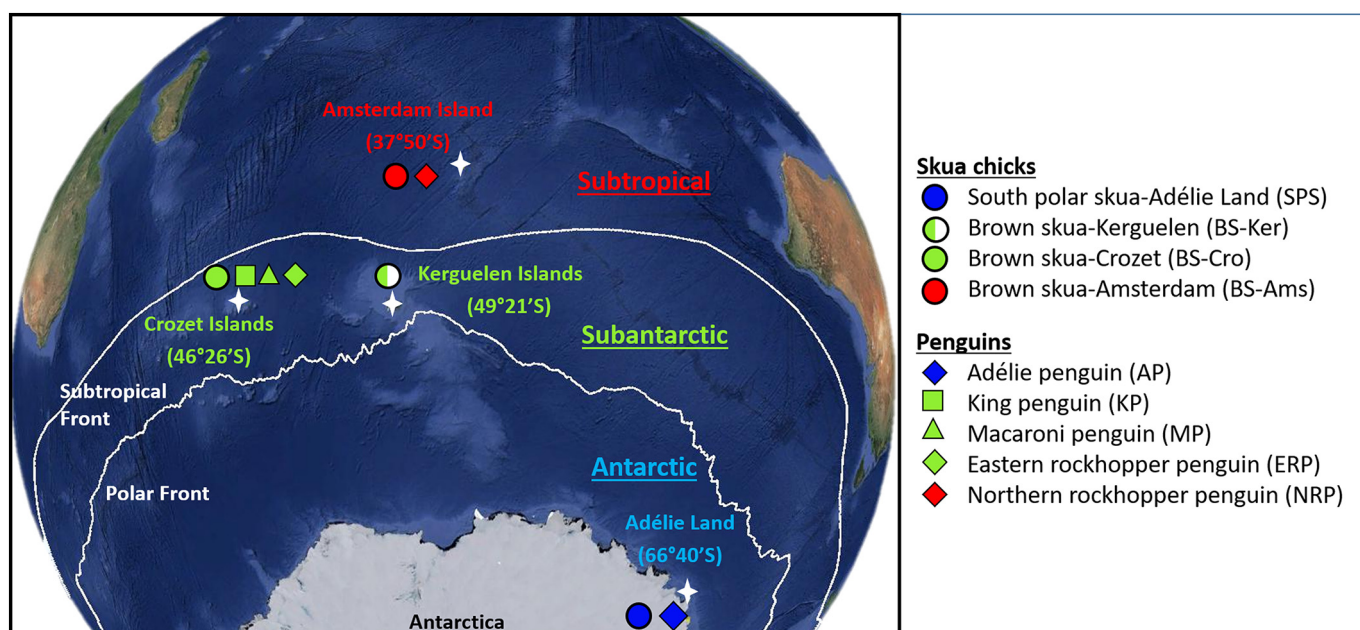


Fig. 1. Bird species, sampling sites and main oceanographic fronts and water masses in the southern Indian Ocean.

variations of Hg isotopic signatures of seabird blood (both MIF and MDF), then providing new insights to better constrain Hg and MeHg cycling in the Southern Ocean and seabird exposure to Hg.

2. Material and methods

2.1. Sample collection and sampling sites

Blood samples were collected during the Austral summer 2011–2012 (from October to February) at the four sites of the Terres Australes et Antarctiques Françaises, from south to north: the high-Antarctic Adélie Land (66°40'S, 140°10'E), the Subantarctic Kerguelen (49°21'S, 70°18'E) and Crozet Islands (46°26'S, 51°45'E), and the Subtropical Amsterdam Island (37°50'S, 77°31'E). Chicks from two species of skuas (the south polar skua *Catharacta maccormicki* in Adélie Land and the brown skua *C. lonnbergi* elsewhere) and adults from five species of penguins (king penguin *Aptenodytes patagonicus*, Adélie *Pygoscelis adeliae*, macaroni *Eudyptes chrysolophus*, eastern rockhopper *E. chrysocome filholi* and northern rockhopper *E. chrysocome moseleyi*) were randomly chosen at the end of the chick-rearing period (Fig. 1). Blood was sampled from the alar vein, and centrifuged to separate the plasma from the blood cells (hereafter blood) which were kept frozen at -20°C . Before the analysis, blood samples were lyophilized with Hg concentrations being reported as dry weight (dw). The dates and localities of the sampling protocol, as well as the ecological characteristics of each seabird species at the various localities are specified in the SI section. Carbon ($\delta^{13}\text{C}$) and nitrogen ($\delta^{15}\text{N}$) stable isotope ratios were determined in blood cells as detailed in previous work (Renedo et al., 2018b).

2.2. Reference materials, sample preparation, and analytical description

2.2.1. Reference samples

To validate the analytical results for Hg speciation, four certified reference materials were analyzed: human hair NIES-13 and IAEA-086; tuna fish ERM-CE-464 and dogfish liver DOLT-4 (Table S1). Hg isotopic results for blood were also validated with these four reference materials by intercomparison with previously reported values (Li et al., 2014; Yamakawa et al., 2016) and with reference values of Lake Michigan fish tissue NIST SRM 1947. Two internal reference samples were also

prepared with the pooled samples collected from different king penguin individuals from Crozet Islands: RBC-KP (red blood cells) and F-KP (feathers) and were analyzed at each analytical session. Analytical uncertainty for delta values was calculated using SD typical errors for reference materials, as recommended by reference publications for standard reporting of Hg isotopic ratio uncertainties (Table S2).

2.2.2. Measurement of the Hg compound concentrations (GC-ICPMS)

For speciation analyses, Hg was extracted from blood (0.10–0.15 g) by alkaline microwave digestion with 5 mL of tetramethylammonium hydroxide (25% TMAH in H_2O , Sigma Aldrich) (Rodrigues et al., 2011; Queipo Abad et al., 2017). The extraction method, analysis, and quantification of Hg species have been detailed previously (Renedo et al., 2018a). Total Hg concentrations were quantified by using an advanced Hg analyzer (AMA-254, Altec). Total Hg concentrations obtained by Hg speciation analyses (i.e., the sum of inorganic and organic Hg) were compared to total Hg concentrations obtained by AMA-254 for method validation. Recoveries of Hg and MeHg concentrations with respect to the certified values for each reference material varied between 96 and 101% (see Table S1 for details).

2.2.3. Measurement of the total Hg isotopic composition by CVG-MC-ICPMS

For isotopic analyses, blood (0.05–0.10 g) was predigested overnight at room temperature and then digested the following day with 3 or 5 mL of HNO_3 acid (65%, INSTRA quality). Samples were subsequently extracted in a Hotblock at 75°C for 8 h (6 h in HNO_3 and >2 h after the addition of 1/3 of the total volume of H_2O_2 (30%, ULTREX quality)). Hg isotopic analyses were carried out as reported previously (Renedo et al., 2018a). Hg isotopic values were reported as delta notation, calculated relative to the bracketing standard NIST SRM-3133 reference material to allow inter-laboratory comparisons, as described in the SI section. NIST SRM-997 thallium standard solution was used for the instrumental mass-bias correction using the exponential law. Secondary standard NIST RM-8160 (previously UM-Almadén standard) was used for validation of the analytical session (Table S2). Total Hg concentrations in the extract solution were compared to the concentrations found by AMA-254 analyses to assess method recovery. The obtained average recovery was $100 \pm 2\%$ ($n = 110$).

2.3. Statistical tests

Statistical analyses were performed using R 3.3.2 software (R Core Team, 2016). Prior to the analyses, the data were checked for normality of the distribution and homogeneity of variances using Shapiro–Wilk and Breusch–Pagan tests, respectively. Non-parametric tests (Kruskal–Wallis with the Conover–Iman test) were performed accordingly. We examined the correlations between MeHg concentrations, Hg MDF ($\delta^{202}\text{Hg}$) and MIF ($\Delta^{199}\text{Hg}$ and $\Delta^{200}\text{Hg}$) with latitude using linear regressions and Spearman correlation rank tests. Statistically significant results were set at $\alpha = 0.05$.

3. Results and discussion

3.1. Total Hg concentrations (THg) and Hg speciation trends

MeHg was the dominant Hg form in the blood of all the individuals ($92 \pm 7\%$, mean \pm SD; Table 1). This means that Hg isotopic composition of blood corresponded essentially to the MeHg isotopic values. Both the skua and penguin blood samples exhibited significantly different MeHg concentrations according to the sites (Kruskal–Wallis, $H = 31.09$ and 43.05 , respectively, both $p < 0.0001$). The skua blood MeHg concentrations increased from 0.51 to $3.78 \mu\text{g}\cdot\text{g}^{-1}$ dw ($n = 40$) from the Antarctic to Subtropical populations, respectively. Concentrations of MeHg in penguin blood were also lower for Antarctic than for Subtropical species (0.43 to $1.95 \mu\text{g}\cdot\text{g}^{-1}$ dw, respectively, $n = 51$), increasing in the order Adélie < eastern rockhopper < macaroni < king < northern rockhopper penguins (Table 1). MeHg concentrations in seabird blood showed a significant correlation with latitude for both skuas (Adjusted $r^2 = 0.62$, $p < 0.0001$) and penguins (Adjusted $r^2 = 0.33$, $p < 0.0001$) (Fig. S1). Previous studies addressed the influence of the intrinsic and extrinsic ecological factors of these two seabird models (age, sex, moulting patterns, diet or feeding habitats) on the latitudinal variations of MeHg concentrations (Carravieri et al., 2016, 2017), as well as the Hg isotopic composition (Renedo et al., 2018a) of blood or feathers at the same study sites. The main factor explaining inter-species differences in Hg levels in a same ecosystem were feeding habits, rather than physiological or taxonomic differences (Carravieri et al., 2014, 2016). However, the influence of the dietary habits did not influence the latitudinal variations of MeHg blood levels, suggesting that the higher seabird MeHg concentrations in Subtropics than in Antarctica depend mainly on the geographical differences of Hg sources and dynamics (Renedo et al., 2018b) or incorporation into food webs (Carravieri et al., 2016).

3.2. Latitudinal trends of Hg stable isotopic composition

A wide range of mean blood $\delta^{202}\text{Hg}$ values was observed between Antarctic and Subtropical populations for both skuas and penguins (0.23 – 1.56% and 0.53 – 2.16% , respectively) (Table 1). The mean variation of $\delta^{202}\text{Hg}$ values of blood between Antarctic and Subtropical sites was $1.33 \pm 0.15\%$ (-0.02 to 1.71%) for skuas and $1.60 \pm 0.25\%$ (0.24 – 2.37%) for penguins. We observed a significant relationship between latitude and $\delta^{202}\text{Hg}$ values of blood for skuas and penguins (Adjusted $r^2 = 0.90$ and 0.85 , respectively, both $p < 0.0001$) (Fig. 2A). $\Delta^{199}\text{Hg}$ values varied slightly between the various sites in skuas (1.51 – 1.76%) and penguins (1.54 – 1.89%). The mean variation of $\Delta^{199}\text{Hg}$ values was $0.25 \pm 0.09\%$ (1.31 – 1.85%) for skuas and $0.36 \pm 0.16\%$ (1.38 – 2.04%) for penguins. The $\Delta^{199}\text{Hg}$ values of blood were also significantly correlated with latitude in skuas (Adj. $r^2 = 0.55$, $p < 0.0001$) and penguins (Adj. $r^2 = 0.18$, $p < 0.0001$) (Fig. 2B). Low differences were observed for the even–MIF signatures (denoted here as $\Delta^{200}\text{Hg}$) between Antarctic ($-0.02 \pm 0.04\%$) and Subtropical populations ($0.04 \pm 0.05\%$). The even–MIF values of Subantarctic seabirds ($0.00 \pm 0.04\%$) were not significantly different from Antarctic seabirds, when skuas and penguins were

Table 1
Total and MeHg concentrations (Mean \pm SD, $\mu\text{g}\cdot\text{g}^{-1}$ dw) and Hg isotopic composition ($\delta^{202}\text{Hg}$, $\Delta^{199}\text{Hg}$ and $\Delta^{200}\text{Hg}$, Mean \pm SD, %) in blood of skua and penguin species. n = number of individuals. Values not sharing the same superscript letter within each group are statistically different. All Hg isotopes as well as C and N isotope composition of each individual are included in Supplementary Tables S12 and S13.

Species	Abbreviations	Location	Diet	Sampling date	n	THg $\mu\text{g}\cdot\text{g}^{-1}$	MeHg $\mu\text{g}\cdot\text{g}^{-1}$	% THg	$\delta^{202}\text{Hg}$ ‰	$\Delta^{199}\text{Hg}$ ‰	$\Delta^{200}\text{Hg}$ ‰
South polar skua	SPS	Adélie Land	penguins	Dec 2011-Jan 2012	9	0.53 ± 0.08^A	0.51 ± 0.09^A	90 ± 4^A	0.23 ± 0.13^A	1.51 ± 0.08^A	-0.01 ± 0.03^A
Brown skua	BS-Ker BS-Cro BS-Amis AP	Kerguelen Crozet Amsterdam Adélie Land	petrels penguins & rats unknown (seabirds, fur seals) pelagic crustaceans & fish	Dec 2011 Jan-Feb 2012 Dec 2011 Feb 2012	10 11 10 10	2.32 ± 0.34^B 1.81 ± 1.19^B 4.00 ± 0.89^C 0.47 ± 0.12^A	2.16 ± 0.33^B 1.70 ± 1.16^B 3.78 ± 0.79^C 0.43 ± 0.11^A	93 ± 2^A 94 ± 3^A 95 ± 4^A 93 ± 7^A	1.04 ± 0.08^B 1.39 ± 0.18^C 1.56 ± 0.08^D 0.56 ± 0.20^A	1.61 ± 0.06^A 1.69 ± 0.11^B 1.76 ± 0.05^B 1.54 ± 0.11^A	0.00 ± 0.04^A 0.02 ± 0.03^A 0.03 ± 0.05^A -0.03 ± 0.05^A
Adélie penguin	KP	Crozet	pelagic fish	Oct 2011	11	2.01 ± 0.29^B	1.88 ± 0.28^B	93 ± 1^A	1.49 ± 0.11^B	1.60 ± 0.04^A	-0.02 ± 0.03^{AB}
King penguin	MP	Crozet	pelagic crustaceans & fish	Jan 2012	10	1.06 ± 0.16^C	1.01 ± 0.15^C	96 ± 2^A	1.66 ± 0.11^C	1.54 ± 0.06^A	0.00 ± 0.04^{AB}
Macaroni penguin	ERP	Crozet	pelagic crustaceans & fish	Feb 2012	10	0.97 ± 0.20^C	0.93 ± 0.19^C	95 ± 1^A	1.93 ± 0.18^D	1.77 ± 0.13^B	0.01 ± 0.07^{AB}
Eastern rockhopper penguin	NRP	Amsterdam	pelagic crustaceans squid & fish	Nov 2011	10	2.40 ± 0.56^B	1.95 ± 0.43^B	82 ± 13^B	2.16 ± 0.14^E	1.89 ± 0.12^B	0.05 ± 0.06^B

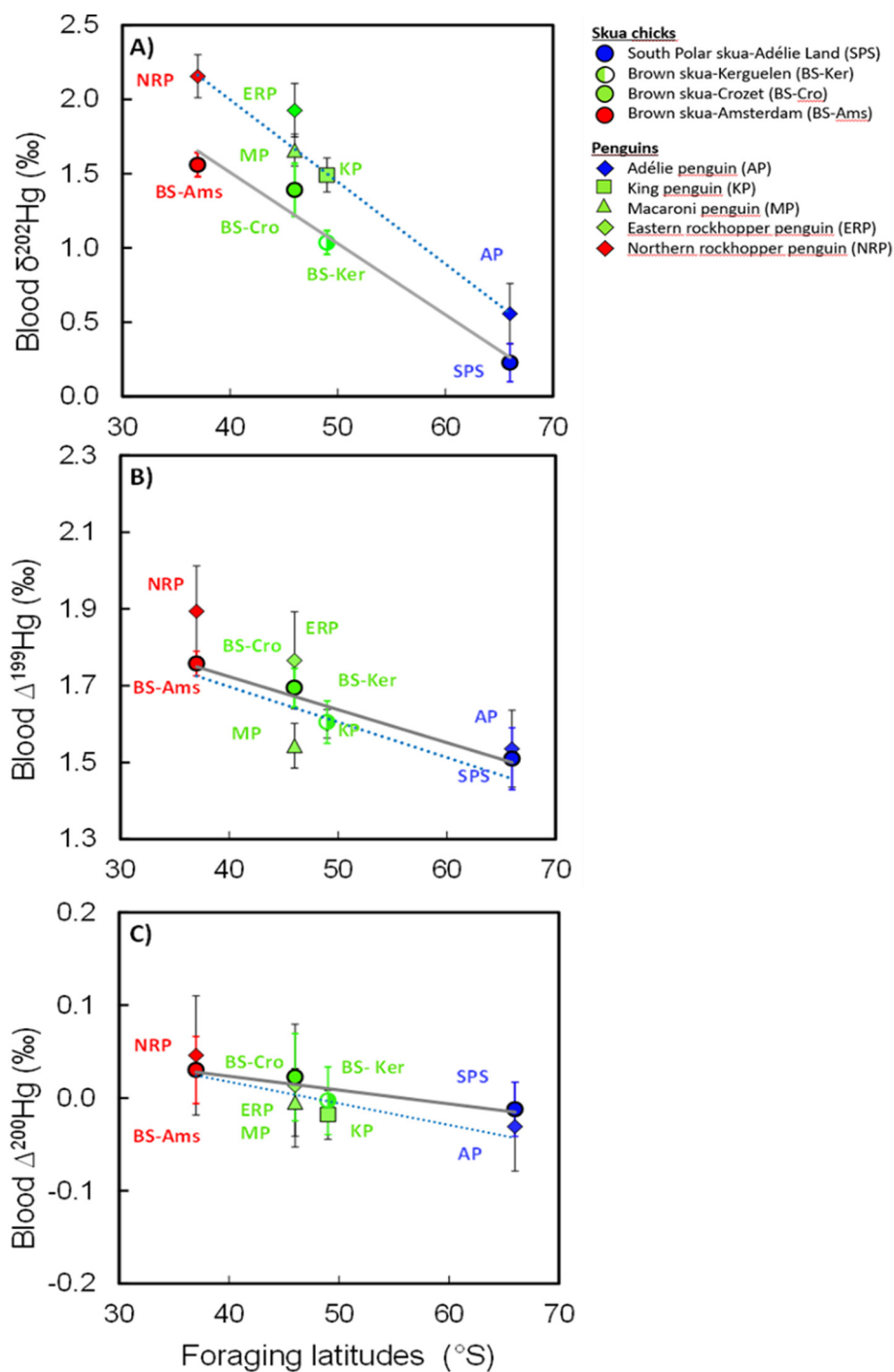


Fig. 2. Blood Hg isotopic composition (mean values \pm SD) of skua chicks and penguin adults from the Southern Ocean versus latitude. The grey line represents the linear regression for skua chicks ($n = 40$) and the blue dotted line is the linear regression for penguins ($n = 51$). A) Regression equations for skua $\delta^{202}\text{Hg}$ blood-latitude ($y = -0.05x + 3.43$, Adj. $r^2 = 0.90$, $p < 0.0001$) and for penguin $\delta^{202}\text{Hg}$ blood-latitude ($y = -0.05x - 4.21$, Adj. $r^2 = 0.85$, $p < 0.0001$). B) Regression equations for skua $\Delta^{199}\text{Hg}$ blood-latitude ($y = -0.01x + 2.07$, Adj. $r^2 = 0.55$, $p < 0.0001$) and for penguin $\Delta^{199}\text{Hg}$ blood-latitude ($y = -0.01x + 2.25$, Adj. $r^2 = 0.17$, $p < 0.0001$). C) Regression equations for skua $\Delta^{200}\text{Hg}$ blood-latitude ($y = -0.0015x + 0.08$, Adj. $r^2 = 0.15$, $p = 0.008$) and for penguin $\Delta^{200}\text{Hg}$ blood-latitude ($y = -0.0023x + 0.12$, Adj. $r^2 = 0.15$, $p = 0.001$). KP is not situated at the Crozet latitude because this species forages at the Polar Front during their breeding period and Hg isotopes of blood are then representative of this zone (Renedo et al., 2018b). (For interpretation of the references to colour in this figure legend, the reader is referred to the web version of this article).

considered together ($H = 13.22$, $p = 0.001$). Although the even-MIF latitudinal variations were low for the two groups of seabirds, they exhibited a significant linear trend with latitude in both skuas (Adj. $r^2 = 0.15$, $p = 0.008$) and penguins (Adj. $r^2 = 0.15$, $p = 0.001$) (Fig. 2C).

The strong relationship of Hg isotopic signatures with latitude (Fig. 2) could be explained by a combined influence of different Hg sources (with different Hg isotopic baselines) and processes

associated with geographically changing conditions that would induce Hg isotopic fractionation across the study sites. In the following sections, we conceptually propose, estimate and discuss the contribution of these potential explanatory factors, from regional atmospheric sources (Hg even-MIF), through sea surface photochemistry (Hg odd-MIF) to biotic dark processes in the water column (additional Hg MDF).

3.3. Regional atmospheric sources potentially affect Hg isotopic baseline in seabirds from distant latitudes of the Southern Ocean

Hg even-MIF ($\Delta^{200}\text{Hg}$) is thought to be associated with mechanisms occurring in the upper atmosphere, and it is not affected by any biogeochemical processes, including photochemical processes in the euphotic zone, as observed so far (Gratz et al., 2010; Chen et al., 2012; Sherman et al., 2012a, 2012b). The $\Delta^{200}\text{Hg}$ values detected in the blood of skuas and penguins exhibited minor variations between the distant latitudes and high variability at the population level (Fig. 2C). We observed higher $\Delta^{200}\text{Hg}$ values in Subtropical seabirds (skuas + penguins) from Amsterdam Island ($0.04 \pm 0.05 \text{ ‰}$), whereas slightly lower $\Delta^{200}\text{Hg}$ values were obtained in Subantarctic ($0.00 \pm 0.04 \text{ ‰}$) and Antarctic seabirds ($-0.02 \pm 0.04 \text{ ‰}$). Our $\Delta^{200}\text{Hg}$ values of seabirds are in the same range to the ones observed in Arctic marine predators of Alaska that also presented a decreasing trend of $\Delta^{200}\text{Hg}$ values with latitude (from 0.10 to -0.01 ‰ ; 53.93 to 71.30°N, Masbou et al., 2018). Interestingly, precipitation samples worldwide generally exhibited an inverse latitudinal gradient, with higher $\Delta^{200}\text{Hg}$ values at high latitudes relative to low latitude regions (Chen et al., 2012; Gratz et al., 2010; Sherman et al., 2012b), which is potentially associated with the shallower troposphere at higher latitudes (Cai and Chen, 2015). The inversed $\Delta^{200}\text{Hg}$ trends between atmospheric samples and biological tissues with latitude highlights the complexity of Hg atmospheric deposition pathways and the necessity of further research exploring Hg isotopes in atmospheric samples in Southern Polar Regions to elucidate the mixed contribution of Hg atmospheric inputs. Although the slight variations of seabird $\Delta^{200}\text{Hg}$ values do not provide conclusive evidence, our close-to-zero data are closer to the values observed in atmospheric total gaseous Hg (-0.11 to -0.01 ‰ , Demers et al., 2013; Sherman et al., 2010). This seems to indicate that the predominant Hg atmospheric source are originating from tropospheric gaseous elemental Hg, which would be oxidized to Hg(II) and deposited as dry or wet deposition, and eventually re-emitted after reduction in surface environment. Recent models in the Arctic Ocean estimated limited uptake of Hg⁰ as a result of ice cover and saturation of surface waters in dissolved Hg⁰ (Soerensen et al., 2016), therefore analogous processes in sea-ice covered regions of Antarctica can be assumed. Though, the sequestration of atmospheric Hg⁰ (and oxidized Hg(II)) in the sea ice compartment in Antarctic zones is thought to be responsible for an additional input of Hg to the ocean (Cossa et al., 2011; Gionfriddo et al., 2016). Moreover, additional processes could transport oxidized Hg(II) from the Antarctic continent to Antarctic coasts by katabatic winds (Angot et al., 2016), also contributing to negative $\Delta^{200}\text{Hg}$ values registered in Antarctic seabird populations. Arctic snowfall impacted by atmospheric depletion events exhibited mostly negative to near-to zero $\Delta^{200}\text{Hg}$ values (-0.12 ‰ , Sherman et al., 2010), therefore we suggest that substantial deposition of oxidized Hg(II) in the Antarctic snowpack and consequent melting of ice could contribute to negative $\Delta^{200}\text{Hg}$ values in the Antarctic ecosystem. Slightly negative $\Delta^{200}\text{Hg}$ values in Antarctic ornithogenic sediments (down to -0.07 ‰ , Zheng et al., 2015) are also close to the relatively negative values registered in our Antarctic seabirds. Indeed, sediment erosion and its mobilization to opened areas could also contribute to Hg release into the aquatic compartment in water masses surrounding the Antarctic continent or the coastal zones in the vicinity of the Subantarctic islands. On the assumption that a higher interaction between coastal sediment and biota is produced in the Antarctic zone near the continent compared to Subantarctic and Subtropical islands, $\Delta^{200}\text{Hg}$ values in Antarctic seabirds breeding in Adélie Land may be also lower relative to Subantarctic and Subtropical communities. However, sediment Hg inputs in coastal waters of the Subantarctic and Subtropical islands are not negligible, since Hg isotopes from the coastal and partly benthic gentoo penguin *Pygoscelis papua* are influenced by sediment-derived Hg at the local scale of the Crozet archipelago (Renedo et al., 2018b).

3.4. Low variability of MeHg photodemethylation extent between distant latitudes of the Southern Ocean

As a significantly positive Hg odd-MIF is thought to be mainly due to the photochemical processes prior to MeHg incorporation into food webs (Bergquist and Blum, 2007), we initially considered that the variability of $\Delta^{199}\text{Hg}$ values of seabirds between the three geographically distant areas (Antarctic, Subantarctic, and Subtropical) (Fig. 2B) could be primarily due to distinct conditions influencing photochemical reactivity in surface waters. Aquatic photochemical MeHg demethylation is known to induce an increase in odd-MIF ($\Delta^{199}\text{Hg}$ and $\Delta^{201}\text{Hg}$) and in MDF values ($\delta^{202}\text{Hg}$) in the residual MeHg pool (Bergquist and Blum, 2007). This process results in a $\Delta^{199}\text{Hg}/\Delta^{201}\text{Hg}$ ratio of 1.36 ± 0.04 , as reported experimentally (Bergquist and Blum, 2007). Meanwhile, experimental photochemical reduction of Hg(II) yielded a $\Delta^{199}\text{Hg}/\Delta^{201}\text{Hg}$ ratio of 1.00 ± 0.01 (Bergquist and Blum, 2007). The $\Delta^{199}\text{Hg}/\Delta^{201}\text{Hg}$ slopes obtained for penguin blood (1.17 ± 0.06 , intercept: -0.07 ± 0.08 , SE) and skua blood (1.14 ± 0.07 , intercept: 0.05 ± 0.11 , SE) (Fig. S2) differed slightly from those obtained from previous photodemethylation laboratory experiments, but they are in good agreement with those previously obtained with marine fish (Senn et al., 2010; Blum et al., 2013) and seabird eggs (Point et al., 2011; Day et al., 2012). The overall $\Delta^{199}\text{Hg}/\Delta^{201}\text{Hg}$ slope for both skuas and penguins was 1.16 ± 0.05 (SE) with negligible intercept (0.01 ± 0.07). Our slopes were also similar to the $\Delta^{199}\text{Hg}/\Delta^{201}\text{Hg}$ ratios obtained in fish from King George Island (1.19 ± 0.17 , $n = 8$; Liu et al., 2019) and faeces from Antarctic seals (1.16 , $n = 2$; Zheng et al., 2015), but slightly lower than ratios reported on Adélie penguin guano (~ 1.30 , $n = 2$; Zheng et al., 2015). The lower $\Delta^{199}\text{Hg}/\Delta^{201}\text{Hg}$ slopes typically observed in marine biota compared to laboratory photochemical experiments can be the consequence of differences in organic matter or the influence of dissolved cations and halogens present in seawater. Recently, other studies have focused on the influence of the type of solar radiation and different ligands in MeHg photodemethylation processes in aquatic systems (Chandan et al., 2015; Rose et al., 2015). Rose et al. (2015) investigated the effect of solar radiation (different intensities and frequencies) on Hg MIF during MeHg aquatic photodemethylation and obtained a ratio similar to Bergquist and Blum (2007). Chandan et al., (2015) documented variable $\Delta^{199}\text{Hg}/\Delta^{201}\text{Hg}$ ratios for MeHg photodemethylation under different types and concentrations of dissolved organic carbon (DOC) ligands with different content of reduced sulfur (S-red). Under low MeHg/S-red-DOC ratios $\Delta^{199}\text{Hg}/\Delta^{201}\text{Hg}$ slopes were consistent and less variable (1.38 ± 0.02); whereas high MeHg/S-red-DOC ratios presented lower slopes varying from 1.17 ± 0.04 to 1.30 ± 0.02 (Chandan et al., 2015).

Assuming that MeHg photodegradation is the dominant photochemical process before MeHg incorporation into food webs, we estimated the fraction of photodemethylated MeHg of each area based on three experimental models (Bergquist and Blum, 2007; Chandan et al., 2015). Although the use of experimental models based on more realistic environmental conditions (low MeHg/Sred-DOC ratios) can be more representative of the processes occurring under natural conditions in the environment, we are conscious of the degree of extrapolation of these models to real environments. Therefore, the isotopic fractionation systems of these models were adjusted to our specific conditions of MeHg/Sred-DOC ratios and MeHg/DOC ratios by fitting equations for the three sites (Antarctic, Subantarctic and Subtropical zones) to maximize the accuracy and veracity of our estimations (Tables S5, S6 and S7). The difference in the extent of photodemethylated MeHg from Antarctic and Subantarctic to Subtropical zones was on the order of 2%, independently of the experimental model used. Taking the closer estimates for MeHg, DOC, and dissolved organic sulfur (DOS) concentrations in the study areas (Bergquist and Blum, 2007; Chandan et al., 2015), the extent of photodemethylated MeHg varied from $\sim 9\%$ in Antarctic to $\sim 11\%$ in Subtropical zones (Table S8). Despite the wide distance between the studied sites, the variation of the extent of MeHg photodemethylation

was surprisingly low. For instance, previous isotopic investigations in open ocean areas reported an extent of MeHg photodemethylation of ~40–80% (Senn et al., 2010; Blum et al., 2013), although the high degree of stratification and low productivity of these oligotrophic opened areas compared to our studied sector of the Southern Ocean can lead to this significant difference. However, our estimated MeHg photodemethylation extents are similar to those calculated in eggs of seabirds of the Arctic Ocean (~8–16%, Point et al., 2011) and in ornithogenic sediment cores of the Antarctic coastal ecosystem (~13–18%; Zheng et al., 2015), using similar calculation models (Chandan et al., 2015). A similar variation of the degree of MeHg photodemethylation was also calculated across the Crozet penguin community between benthic (13%) and epipelagic (16%) foragers (Renedo et al., 2018b) also estimated using similar calculation models (Bergquist and Blum, 2007; Chandan et al., 2015). Also, Blum et al. (2013) found that the fish $\Delta^{199}\text{Hg}$ values of the MeHg in mesopelagic fish of the Pacific Ocean were about 1.5–2.0‰, i.e. within the same range as $\Delta^{199}\text{Hg}$ values for seabirds in our study.

Based on the previous observations of Hg isotopes of penguins from Crozet Islands (Renedo et al., 2018b) and on the variations observed of Hg odd-MIF as a function of the foraging depth of marine fish (Blum et al., 2013), the low degree and the minor variations of MeHg photodegradation in distant sites of the Southern Ocean strongly suggest that the major proportion of the MeHg that accumulated in the seabirds was minimally photodemethylated, thus primarily originating from dark environments. Moreover, maximum MeHg concentrations in the open ocean water column are commonly observed at areas with minimum oxygen levels (Monperrus et al., 2007; Kirk et al., 2008; Sunderland et al., 2009; Cossa et al., 2009), including in the Southern Ocean (Cossa et al., 2011). These observations demonstrated active MeHg production and accumulation in organisms from such environments (e.g., Chauvelon et al., 2012). Substantial deep net Hg methylation can be supported by a larger export of organic matter (Sokolov, 2008; Sullivan et al., 1993), subsequent larger inorganic Hg substrate supply (Cossa et al., 2011) from the euphotic zone (<60 m depth;

Tripathy et al., 2015) to mesopelagic waters, and MeHg preservation from photodegradation (Monperrus et al., 2007; Heimbürger et al., 2015). Therefore, the existence of substantial net methylation occurring at depth suggests that the MeHg accumulated in seabirds from the Southern Ocean was predominantly of mesopelagic origin. Further, the lower $\Delta^{199}\text{Hg}/\Delta^{201}\text{Hg}$ slopes of seabirds compared to previous studies (i.e. Blum et al., 2013) also suggest potential export of surface Hg(II) to mesopelagic environments where it is methylated. Due to the high intensity of winter cooling and the seasonal mixed layer depths oscillations, the vertical transport of MeHg and Hg(II) between shallow and deep-water masses could be a preponderant factor explaining the low extent of photochemical processes over these oceanic regions.

3.5. Major variations of the Hg isotopic composition between distant latitudes indicate distinct regional biogenic transformation and bioaccumulation extent

3.5.1. Trophic transfer and accumulation

The strong correlation between the $\Delta^{199}\text{Hg}$ and the $\delta^{202}\text{Hg}$ values of both skuas and penguins (Adj. $r^2 = 0.76$ and 0.61 , respectively, both $p < 0.0001$; Fig. S3) could be indicative of different sources of Hg with distinct isotopic signatures (MDF and MIF) and/or different processes before Hg incorporation or during uptake and bioaccumulation in the food web that produce both Hg MDF and MIF across the different sites. By calculation of the corresponding latitudinal differences of $\delta^{202}\text{Hg}$ obtained experimentally for photochemical demethylation (Chandan et al., 2015), we estimated that approximately 0.3‰ of the total $\delta^{202}\text{Hg}$ variation may be induced by photochemical MeHg breakdown (Tables S9 and S10). This means that the remaining 1.0–1.3‰ of $\delta^{202}\text{Hg}$ differences between latitudes may be the consequence of various Hg sources and/or biogeochemical processes inducing a reservoir of isotopically heavier Hg in the Subtropical region (Fig. 3).

The Antarctic ecosystem is characterized by a less complex food web in which top predators feed mainly on a limited number of key available species, such as the Antarctic krill *Euphausia superba* (Cherel, 2008;

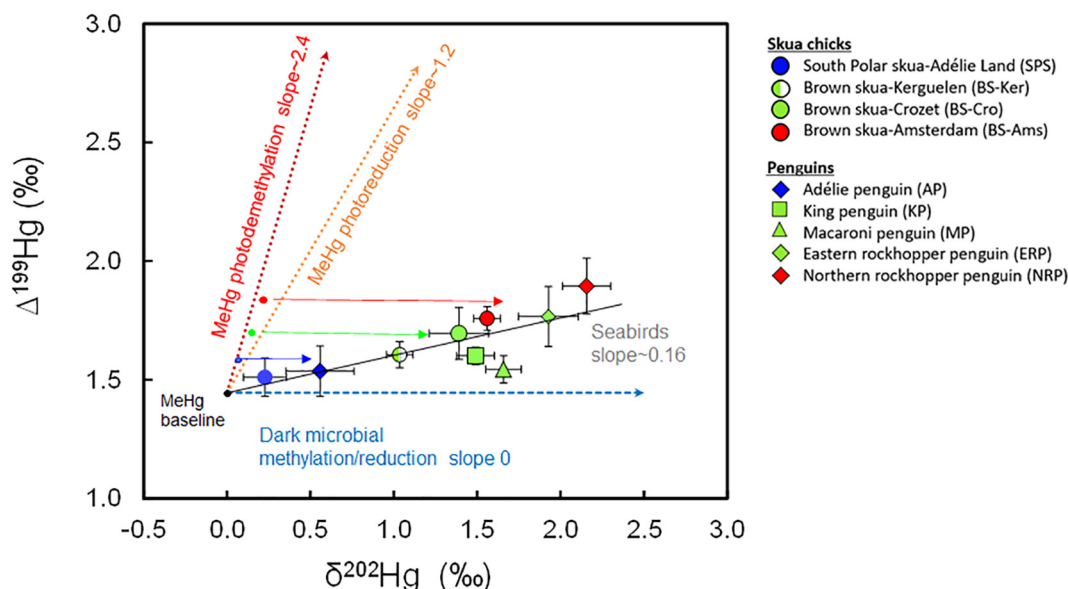


Fig. 3. Blood odd-MIF ($\Delta^{199}\text{Hg}$) versus MDF ($\delta^{202}\text{Hg}$) of skua chicks ($n = 40$) and penguin adults ($n = 51$) from the Southern Ocean (means \pm SD). The regression equation for MIF versus MDF slope of the overall data (skuas + penguins) is $y = 0.16x + 1.44$, Adj. $r^2 = 0.40$, $p < 0.0001$. Theoretical slopes for photochemical demethylation and reduction are taken from experimental studies (Bergquist and Blum, 2007). Since microbial Hg transformations do not induce Hg MIF, slopes for dark biotic methylation/reduction are considered to be zero (Kritee et al., 2007, 2009). This illustration represents the isotopic fractionation from the primary MeHg source (black point) through the MeHg accumulated in seabirds. The isotopic baseline of the Hg source is influenced by both photochemical demethylation and reduction processes before assimilation in the food web (following a slope between 2.4 and 1.2). The different extent of photochemical processes between Antarctic (blue), Subantarctic (green) and Subtropical waters (red) leads to different odd-MIF extent (and associated MDF) between latitudes. Once the MeHg is assimilated in the food web, the different extent of Hg biological transformations (i.e. methylation/demethylation/reduction) will induce additional MDF while the $\Delta^{199}\text{Hg}$ signatures remain constant. Fig. S3 shows the individual blood Hg MIF versus MDF values of all the analyzed seabirds. (For interpretation of the references to colour in this figure legend, the reader is referred to the web version of this article).

Brasso et al., 2014). By contrast, Subantarctic and Subtropical ecosystems have a larger diversity of prey species including four species of Euphausiids (Cherel et al., 2007; Bost et al., 2009), constituting more complex food webs. Therefore, the difference in food web complexity between the studied sites could explain the increasing MeHg levels from Antarctic to Subtropical ecosystems (Lavoie et al., 2013). However, such difference in the marine trophic transfer of MeHg was not yet found to induce any significant variations of $\delta^{202}\text{Hg}$. Trophic processes do not appear to explain the total MDF variation, because both seabird models with contrasting trophic ecologies exhibited the same MDF variations between the different latitudes and similar associated slopes. Indeed, although higher blood Hg concentrations were obtained in skua chicks relative to adult penguins at each locality, skuas exhibited lower $\delta^{202}\text{Hg}$ values despite their higher trophic level (Carravieri et al., 2014). Since the two different seabird species have contrasted foraging ecology, different MDF values would be expected due to distinct foraging habitats, trophic levels, and consequently different level of exposure to MeHg. Different extent of metabolic processes due to both age status and species-specific characteristics can also lead to significant MDF variations among seabirds. The lower MDF values in seabird chicks could be therefore potentially explained if metabolic processes are less efficient due to their age. This would induce lower *in vivo* Hg isotopic fractionation, thereby leading to lower blood $\delta^{202}\text{Hg}$ values compared to adult penguins. To check this hypothesis, we investigated skua adult blood from the Kerguelen population, for which significantly higher $\delta^{202}\text{Hg}$ values (a mean $\sim 0.54\%$ difference) were observed compared to chicks,

and which also matched with the penguins' MDF-latitude slope (Fig. S4). This observation suggested that the difference in $\delta^{202}\text{Hg}$ values between the two models may be due to a specific metabolic response related to age and/or species, while the latitudinal variation remains mostly independent of such internal biotic pathways. This conclusion agrees with those of previous studies in marine fish (Kwon et al., 2012; Blum et al., 2013) in which trophic effects were found to be independent of Hg isotopic trends and did not significantly affect Hg MDF. Variations in $\delta^{202}\text{Hg}$ values between seabird species of the same ecosystem can be dependent on the Hg sources associated with different integration times between tissues (Renedo et al., 2018a) or specific foraging ecologies (Renedo et al., 2018b). However, the consistent variations of seabird MDF signatures between the different latitudes suggest that a process driven by kinetic isotope fractionation operating at large/regional scales could be the main driver of Hg isotopic geographical variations. In light of this, we have proposed and tested several potential major biogeochemical processes that could drive the observed variations of Hg MDF in seabirds from the four sites (Fig. 4).

3.5.2. Biotic reduction and volatilization

First, we postulated that the higher surface temperature of Subtropical seawaters compared to Antarctic waters could result in a greater degree of biotic reduction and volatilization of inorganic Hg^0 from the aquatic compartment to the atmosphere, thereby leading to a residual pool of isotopically heavier $\text{Hg}(\text{II})$ in the aqueous phase. To test this hypothesis, previous experimental results were used to estimate the

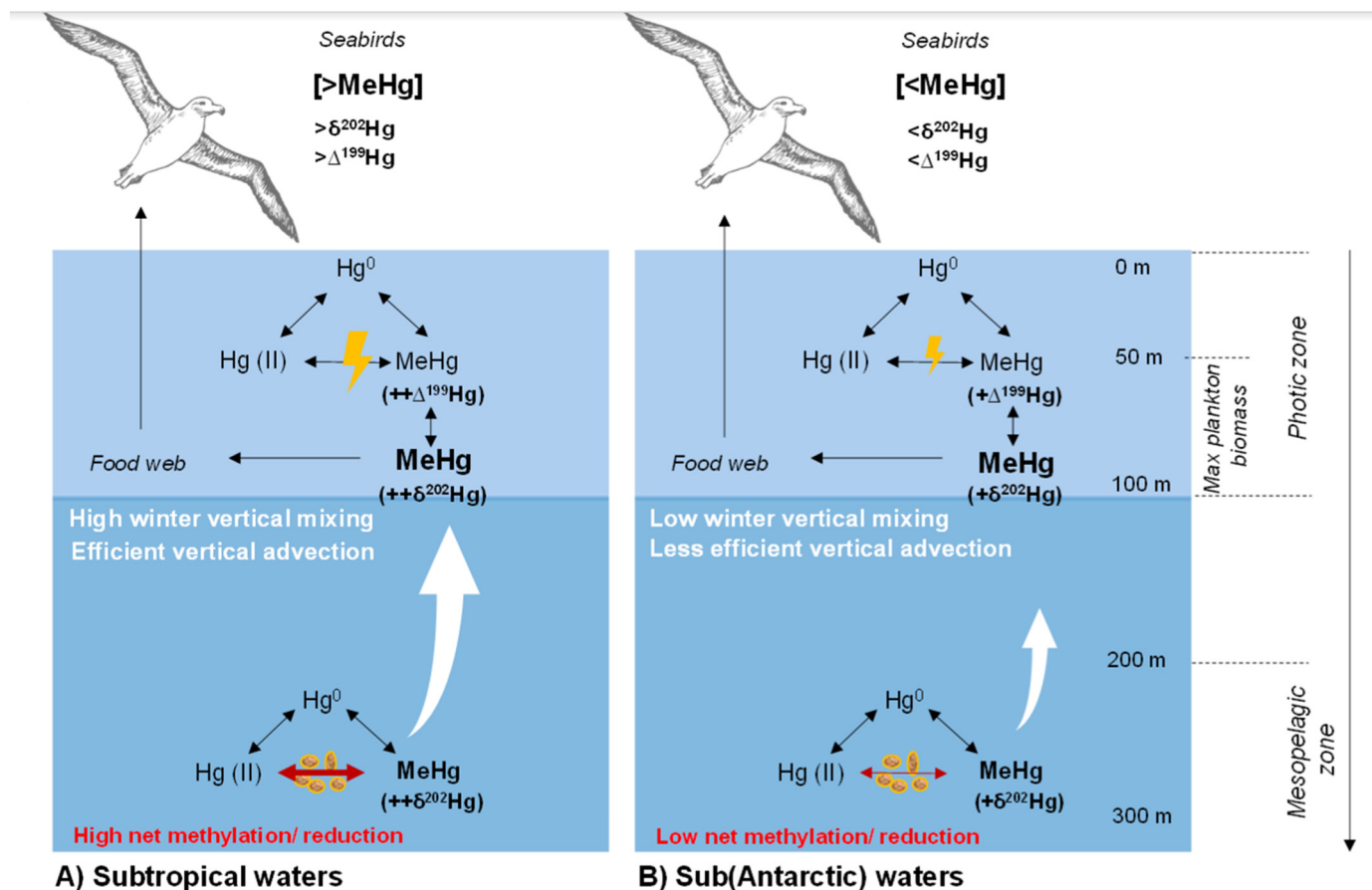


Fig. 4. Schematic illustration of the major processes explaining the Hg isotopic variations between Antarctic, Subantarctic and Subtropical ecosystems of the Southern Ocean. MeHg accumulated in seabirds from these remote regions of the Southern Ocean has a dominant mesopelagic origin. During periods of maximum primary productivity (phytoplankton blooms), a higher net Hg methylation efficiency at depth in subtropical waters together with more efficient winter vertical mixing could favor the transfer of nutrients and newly formed mesopelagic MeHg to the surface. Therefore, MeHg with higher $\delta^{202}\text{Hg}$ values is accumulated in Subtropical food webs (Scenario A). In contrast, lower net microbial methylation in Antarctic and Subantarctic mesopelagic ecosystems with lower vertical advection may indicate less efficient nutrient and MeHg transport to shallower productive zones, explaining the lower $\delta^{202}\text{Hg}$ signatures of bioaccumulated MeHg in Antarctic and Subantarctic food webs. (Scenario B).

variation in the extent of Hg volatilization and Hg biotic reduction from Antarctic to Subtropical waters. By considering the specific conditions of water temperature recorded on the approximate latitudinal sites (Cossa et al., 2011; Canário et al., 2017) and calculation of Henry's law constant reported by experimental studies in seawater (Andersson et al., 2008), we estimated that volatilization can only contribute to 0.03 ‰ of the MDF variation (Table S11). Thus, a different degree of volatilization itself is not enough to explain the total Hg MDF variations across the investigated latitudinal gradient. Based on experimental models for Hg dark bacterial reduction (Kritee et al., 2007, 2008), estimations showed that the extent of biological reduction in Subtropical waters should be on the order of 1.5 to 3 times higher than in Antarctic waters during the summer period to explain the observed MDF variations between regions (Table S12). However, such a high degree of variation in the dark biological reduction rate in the studied oceanic regions should be taken with caution since it cannot be demonstrated by any robust dataset in these regions of the Southern Ocean. Since most of the MeHg that bioaccumulates in seabird tissues seems to originate from the mesopelagic zone (see above), Hg(II) dark biological reduction cannot be discarded, while the environmental conditions are also supposed to be favorable to the formation of MeHg (Sullivan et al., 1993; Cossa et al., 2011). Moreover, we cannot rule out that $\delta^{202}\text{Hg}$ of MeHg would follow a similar trend after various methylation and demethylation steps.

3.5.3. Biotic net Hg methylation and uptake

As a second hypothesis, we postulated that higher MeHg concentrations in Subtropical seabirds could possibly be the result of greater net biotic methylation taking place in the mesopelagic zone. We refer here as "net" methylation extent to the combination of simultaneous methylation and demethylation processes. An increase in the methylation/demethylation ratio from Antarctic to Subtropical zones could also be in agreement with the isotopically heavier residual pool of MeHg (i.e., assuming a steady state) in Subtropical zones. Based on experimental measurements of Hg isotopic fractionation during net MeHg methylation under abiotic (Jiménez-Moreno et al., 2013) and biotic (Perrot et al., 2015) conditions, the net degree of methylation should be on the order of 1.5 to 2.5 times higher in Subtropical waters compared to Antarctic waters (Table S13). Although estimates are based on closed system experiments, it is assumed to be equivalent to the processes occurring in diffusion-limited microenvironments within an open system such as the open ocean. The theoretical magnitude of MDF enrichment during net methylation could thus largely explain the observed MDF latitudinal variation across the studied areas. Indeed, potentially increasing net methylation rates from Antarctic to Subtropical zones are very much in line with both the Hg isotopic latitudinal trends and the higher MeHg levels found in Subtropical seabirds compared to those from Antarctica. Latitudinal variations of MeHg concentrations and Hg isotopic signatures of seabird blood are likely the result of spatial differences in the MeHg production and degradation rates, especially in the darker mesopelagic zone, as suggested by the degree of Hg odd-MIF.

Due to the complex processes of MeHg production and bioaccumulation, the correlation between abiotic MeHg concentrations in seawater and MeHg levels in biota is rarely found in marine ecosystems. The existence of clearly distinct bioregions in the Southern Ocean in terms of vertical profiles of phytoplanktonic biomass and the seasonality of bloom timing is closely related to seasonal fluctuations in vertical oceanic dynamics and light irradiance availability (Ardyna et al., 2017). These factors would clearly affect MeHg production and transport in the water column. Recent Hg isotopic investigations in the North Pacific Subtropical Gyre highlighted that the bioaccumulation of MeHg is strongly linked to the vertical mobilization of Hg with marine sinking particles and by vertical migration of zooplankton (Motta et al., 2019). In the Southern Ocean, an increasing delay in phytoplankton blooms occurs from Subtropical (October) to Subantarctic latitudes (November/December) to Antarctic latitudes (January/February) (Ardyna et al., 2017). Since the bloom periods at each site occurred before or during

our sample collection periods during the Austral summer of 2011–2012 (Table S14), the MeHg integration time in seabird blood corresponded to the stage of maximal primary productivity at each sampling site. The seasonal release of nutrients and algal blooms during austral summer (Sullivan et al., 1993; Sokolov and Rintoul, 2007), enhanced by sea-ice melting in Antarctic coastal zones (Sokolov and Rintoul, 2007; Riaux-Gobin et al., 2013), induce a higher productivity in Antarctic and Polar Front zones. This biomass dilution of Hg could then contribute to lower Hg levels accumulated in Antarctic final predators.

Latitudinal and regional differences in the seasonal dynamics and the oceanic vertical exchange of water masses have been observed in the upwelling branch of the Southern Ocean (Marshall and Speer, 2012). The seasonal variability of the mixed layer depth is substantial in all the sectors of the Southern Ocean (Sallée et al., 2010). During summertime, the mixed layer depth in the vicinity of the Antarctic Circumpolar Current reaches about 100 m (Sallée et al., 2010). The water column is destabilized during winter cooling and the mixed layer deepens, finding its maxima at the north of the Antarctic Circumpolar Current, where the amplitude of the seasonal cycle can exceed 400 m, particularly in the Indian sector (Sallée et al., 2010). We therefore suggest, as illustrated in Fig. 4, that these regional dynamics could be potential key factors influencing the efficiency of the vertical transport of MeHg between deeper mesopelagic waters and surface waters within the euphotic zone (Cossa et al., 2011; Sallée et al., 2010). Deeper mixed layer depths in the north of the Antarctic Circumpolar Current compared to Antarctic waters indicate weaker stratification and deeper vertical mixing at northern Subtropical waters. A shallower winter vertical mixing at Antarctic and Subantarctic waters near the Polar Front could inhibit the downward transport of Hg to deeper pelagic zones, where net methylation should take place. This would also restrain the upward transfer of nutrients and newly formed MeHg at depth and reduce its uptake by phytoplankton and accumulation along the food web. By contrast, a deeper winter mixed layer depth and higher vertical advection to the surface in Subtropical waters should provide efficient downward transport of Hg and subsequent upward transfer of nutrients and MeHg to the productive euphotic zone. As a result, a complex interplay between MeHg formation at depth and winter mixed layer dynamics may contribute to more efficient vertical MeHg upload in Subtropical waters compared to Subantarctic and Antarctic waters. The higher MeHg exposure observed in Subtropical seabirds may, therefore, be the consequence of both greater microbial formation of MeHg and its vertical transport towards the plankton biomass in Subtropical productive zones.

4. Conclusion

The deductions listed above lead to the conclusion that the variability of Hg isotopic signatures among Antarctic to Subtropical seabirds are strongly influenced by both the specific oceanic dynamics and biological productivity turnover from the three contrasted bioregions of the Southern Ocean. Slight variability of Hg odd-MIF isotopic signatures ($\Delta^{199}\text{Hg}$) between Antarctic and Subtropical seabirds strongly suggests that the MeHg accumulated in trophic webs from the Southern Ocean has a dominant mesopelagic origin. Significant variability of MDF Hg isotopic signatures ($\delta^{202}\text{Hg}$) and its correlation to MeHg concentrations in seabirds from the three studied latitudes demonstrates how regional Southern Ocean dynamics and productivity control marine MeHg biogeochemistry and the exposure of seabirds to Hg contamination. Indeed, the investigation of $\delta^{202}\text{Hg}$ latitudinal variability help elucidate the observed increasing MeHg exposure of seabirds from Antarctic to Subtropical waters by an increasing effect of specific biogenic Hg pathways from Antarctic to Subtropical waters, such as Hg biological transformations and accumulation. This study is the first large scale report of Hg isotopic composition in marine organisms from the Southern Ocean and highlights the potential of seabirds to cover for the first

time these wide geographic ranges to document Hg isotopic variations at the ocean scale. However, complementary Hg isotopic studies in these isolated regions are essential to deeply understand the processes driving Hg isotope variations in these ecosystems.

CRediT authorship contribution statement

Marina Renedo: Methodology, Visualization, Writing - original draft, Writing - review & editing. **Paco Bustamante:** Conceptualization, Supervision, Validation, Writing - review & editing. **Yves Cherel:** Conceptualization, Writing - review & editing. **Zoyne Pedrero:** Writing - review & editing. **Emmanuel Tessier:** Methodology, Supervision, Resources. **David Amouroux:** Conceptualization, Supervision, Validation, Writing - review & editing.

Declaration of competing interest

The authors declare that they have no known competing financial interests or personal relationships that could have appeared to influence the work reported in this paper.

Acknowledgements

The authors wish to thank the fieldworkers who helped collecting blood samples. This study received financial and logistical support from the Institut Polaire Français Paul Emile Victor (IPEV, program no. 109, H. Weimerskirch), the French Southern and Antarctic Lands, and by the Agence Nationale de la Recherche (ANR, program POLARTOP, O. Chastel). Special thanks are due to A. Carravieri who managed the sample database. We also wish to thank Prof. S. Blain (UPMC) for fruitful discussions and help with the oceanographic interpretation of our data. The present work was supported financially by the Région Poitou-Charentes (now the Région Nouvelle Aquitaine) through a Ph.D. scholarship to MR, and by the French national program EC2CO Biohefect/Ecodyn/Dril/MicrobiEen (TIMOTAAF project, P.I. D. Amouroux). The IUF (Institut Universitaire de France) is also acknowledged for its support to PB as a senior member.

Appendix A. Supplementary data

Supplementary data to this article can be found online at <https://doi.org/10.1016/j.scitotenv.2020.140499>.

References

Andersson, M.E., Gårdfeldt, K., Wängberg, I., Strömberg, D., 2008. Determination of Henry's law constant for elemental mercury. *Chemosphere* 73, 587–592. <https://doi.org/10.1016/j.chemosphere.2008.05.067>.

Angot, H., Dion, I., Vogel, N., Legrand, M., Magand, O., Dommergue, A., 2016. Multi-year record of atmospheric mercury at Dumont d'Urville, East Antarctic coast: continental outflow and oceanic influences. *Atmos. Chem. Phys.* 16, 8265–8279. <https://doi.org/10.5194/acp-16-8265-2016>.

Ardyna, M., Claustre, H., Sallée, J., D Ovidio, F., Gentili, B., van Dijken, G., D Ortenzio, F., Arrigo, K.R., 2017. Delineating environmental control of phytoplankton biomass and phenology in the Southern Ocean. *Geophys. Res. Lett.*, 5016–5024 <https://doi.org/10.1002/2016GL072428>.

Bearhop, S., Ruxton, G.D., Furness, R.W., 2000. Dynamics of mercury in blood and feathers of great skuas. *Environ. Toxicol. Chem.* 19 (6), 1638–1643. <https://doi.org/10.1002/etc.5620190622>.

Becker, P.H., Goutner, V., Ryan, P.G., González-Solis, J., 2016. Feather mercury concentrations in Southern Ocean seabirds: variation by species, site and time. *Environ. Pollut.* 216, 253–263. <https://doi.org/10.1016/j.envpol.2016.05.061>.

Bergquist, B.A., Blum, J.D., 2007. Mass-dependent and -independent fractionation of Hg isotopes by photoreduction in aquatic systems. *Science* 318, 417–420. <https://doi.org/10.1126/science.1148050>.

Blévin, P., Carravieri, A., Jaeger, A., Chastel, O., Bustamante, P., Cherel, Y., 2013. Wide range of mercury contamination in chicks of southern ocean seabirds. *PLoS One* 8, e54508. <https://doi.org/10.1371/journal.pone.0054508>.

Blum, J.D., Popp, B.N., Drazen, J.C., Anela Choy, C., Johnson, M.W., 2013. Methylmercury production below the mixed layer in the North Pacific Ocean. *Nat. Geosci.* 6, 879–884. <https://doi.org/10.1038/ngeo1918>.

Blum, J.D., Sherman, L.S., Johnson, M.W., 2014. Mercury isotopes in Earth and environmental sciences. *Annu. Rev. Earth Planet. Sci.* 42, 249–269. <https://doi.org/10.1146/annurev-earth-050212-124107>.

Bost, C. a, Thiebot, J.B., Pinaud, D., Cherel, Y., Trathan, P.N., 2009. Where do penguins go during the inter-breeding period? Using geolocation to track the winter dispersion of the macaroni penguin. *Biol. Lett.* 5, 473–476. <https://doi.org/10.1098/rsbl.2009.0265>.

Bowman, K.L., Lamborg, C.H., Agather, A.M., 2020. A global perspective on mercury cycling in the ocean. *Sci. Total Environ.* 710, 136166. <https://doi.org/10.1016/j.scitotenv.2019.136166>.

Brasso, R.L., Chiaradia, A., Polito, M.J., Raya Rey, A., Emslie, S.D., 2014. A comprehensive assessment of mercury exposure in penguin populations throughout the southern hemisphere: using trophic calculations to identify sources of population-level variation. *Mar. Pollut. Bull.* 97, 408–418. <https://doi.org/10.1016/j.marpolbul.2015.05.059>.

Bustamante, P., Carravieri, A., Goutte, A., Barbraud, C., Delord, K., Chastel, O., Weimerskirch, H., Cherel, Y., 2016. High feather mercury concentrations in the wandering albatross are related to sex, breeding status and trophic ecology with no demographic consequences. *Environ. Res.* 144, 1–10. <https://doi.org/10.1016/j.envres.2015.10.024>.

Cai, H., Chen, J., 2015. Mass-independent fractionation of even mercury isotopes. *Sci. Bull.* 61, 116–124. <https://doi.org/10.1007/s11434-015-0968-8>.

Canário, J., Santos-Echeandía, J., Padeiro, A., Amaro, E., Strass, V., Klaas, C., Hoppema, M., Ossebaar, S., Koch, B.P., Laglera, L.M., 2017. Mercury and methylmercury in the Atlantic sector of the Southern Ocean. *Deep. Res. Part II* 138, 52–62. <https://doi.org/10.1016/j.dsr2.2016.07.012>.

Carravieri, A., Bustamante, P., Churlaud, C., Cherel, Y., 2013. Penguins as bioindicators of mercury contamination in the Southern Ocean: birds from the Kerguelen Islands as a case study. *Sci. Total Environ.* 454–455, 141–148. <https://doi.org/10.1016/j.scitotenv.2013.02.060>.

Carravieri, A., Cherel, Y., Blévin, P., Brault-Favrou, M., Chastel, O., Bustamante, P., 2014. Mercury exposure in a large subantarctic avian community. *Environ. Pollut.* 190, 51–57. <https://doi.org/10.1016/j.envpol.2014.03.017>.

Carravieri, A., Cherel, Y., Jaeger, A., Churlaud, C., Bustamante, P., 2016. Penguins as bioindicators of mercury contamination in the southern Indian Ocean: geographical and temporal trends. *Environ. Pollut.* 213, 195–205. <https://doi.org/10.1016/j.envpol.2016.02.010>.

Carravieri, A., Cherel, Y., Brault-Favrou, M., Churlaud, C., Peluhet, L., Labadie, P., Budzinski, H., Chastel, O., Bustamante, P., 2017. From Antarctica to the subtropics: contrasted geographical concentrations of selenium, mercury, and persistent organic pollutants in skua chicks (*Catharacta spp.*). *Environ. Pollut.* 228, 464–473. <https://doi.org/10.1016/j.envpol.2017.05.053>.

Carravieri, A., Bustamante, P., Labadie, P., Budzinski, H., Chastel, O., Cherel, Y., 2020. Trace elements and persistent organic pollutants in chicks of 13 seabird species from Antarctica to the subtropics. *Environ. Int.* 134, 105225. <https://doi.org/10.1016/j.envint.2019.105225>.

Chandan, P., Ghosh, S., Bergquist, B.A., 2015. Mercury isotope fractionation during aqueous photoreduction of monomethylmercury in the presence of dissolved organic matter. *Environ. Sci. Technol.* 49, 259–267. <https://doi.org/10.1021/es503455j>.

Chen, J., Hintelmann, H., Feng, X., Dimock, B., 2012. Unusual fractionation of both odd and even mercury isotopes in precipitation from Peterborough, ON, Canada. *Geochim. Cosmochim. Acta* 90, 33–46. <https://doi.org/10.1016/j.gca.2012.05.005>.

Cherel, Y., 2008. Isotopic niches of emperor and Adélie penguins in Adélie Land, Antarctica. *Mar. Biol.* 154, 813–821. <https://doi.org/10.1007/s00227-008-0974-3>.

Cherel, Y., Hobson, K.A., Guinet, C., Vanpe, C., 2007. Stable isotopes document seasonal changes in trophic niches and winter foraging individual specialization in diving predators from the Southern Ocean. *J. Anim. Ecol.* 76, 826–836. <https://doi.org/10.1111/j.1365-2656.2007.01238.x>.

Cherel, Y., Barbraud, C., Lahournat, M., Jaeger, A., Jaquet, S., Wanless, R.M., Phillips, R.A., Thompson, D.R., Bustamante, P., 2018. Accumulate or eliminate? Seasonal mercury dynamics in albatrosses, the most contaminated family of birds. *Environ. Pollut.* 241, 124–135. <https://doi.org/10.1016/j.envpol.2018.05.048>.

Chouvelon, T., Spitz, J., Caurant, F., Mèndez-Fernandez, P., Autier, J., Lassus-Débat, A., Chappuis, A., Bustamante, P., 2012. Enhanced bioaccumulation of mercury in deep-sea fauna from the Bay of Biscay (north-east Atlantic) in relation to trophic positions identified by analysis of carbon and nitrogen stable isotopes. *Deep. Res. Part I Oceanogr. Res. Pap.* 65, 113–124. <https://doi.org/10.1016/j.dsr.2012.02.010>.

Cossa, D., Averty, B., Pirrone, N., 2009. The origin of methylmercury in open Mediterranean waters. *Limnol. Oceanogr.* 54, 837–844. <https://doi.org/10.4319/lo.2009.54.3.0837>.

Cossa, D., Heimbürger, L.-E., Lannuzel, D., Rintoul, S.R., Butler, E.C.V., Bowie, A.R., Averty, B., Watson, R.J., Remenyi, T., 2011. Mercury in the Southern Ocean. *Geochim. Cosmochim. Acta* 75, 4037–4052. <https://doi.org/10.1016/j.gca.2011.05.001>.

Day, R.D., Roseaneau, D.G., Berail, S., Hobson, K.A., Donard, O.F.X., Vander Pol, S.S., Pugh, R.S., Moors, A.J., Long, S.E., Becker, P.R., 2012. Mercury stable isotopes in seabird eggs reflect a gradient from terrestrial geogenic to oceanic mercury reservoirs. *Environ. Sci. Technol.* 46, 5327–5335. <https://doi.org/10.1021/es2047156>.

Demers, J.D., Blum, J.D., Zak, D.R., 2013. Mercury isotopes in a forested ecosystem: implications for air-surface exchange dynamics and the global mercury cycle. *Glob. Biogeochem. Cycles* 27, 222–238. <https://doi.org/10.1002/gbc.20021>.

Eagles-Smith, C.A., Silbergeld, E.K., Basu, N., Bustamante, P., Diaz-Barriga, F., Hopkins, W.A., Kidd, K.A., Nyland, J.F., 2018. Modulators of mercury risk to wildlife and humans in the context of rapid global change. *Ambio* 47, 170–197. <https://doi.org/10.1007/s13280-017-1011-x>.

Fitzgerald, W.F., Lamborg, C.H., Hammerschmidt, C.R., 2007. Marine biogeochemical cycling of mercury. *Chem. Rev.* 107, 641–662. <https://doi.org/10.1021/cr050353m>.

- Furness, R.W., Camphuysen, C.J., 1997. Seabirds as monitors of the marine environment. *ICES J. Mar. Sci.* 54, 726–737. <https://doi.org/10.1006/jmsc.1997.0243>.
- Gionfriddo, C.M., Tate, M.T., Wick, R.R., Schultz, M.B., Zemla, A., Thelen, M.P., Schofield, R., Krabbenhoft, D.P., Holt, K.E., Moreau, J.W., 2016. Microbial mercury methylation in Antarctic Sea ice. *Nat. Microbiol.* 1, 16127. <https://doi.org/10.1038/nmicrobiol.2016.127>.
- Goutte, A., Barbraud, C., Meillere, A., Carravieri, A., Bustamante, P., Labadie, P., Budzinski, H., Delord, K., Cherel, Y., Weimerskirch, H., Chastel, O., 2014a. Demographic consequences of heavy metals and persistent organic pollutants in a vulnerable long-lived bird, the wandering albatross. *Proc. R. Soc. B Biol. Sci.* 281. <https://doi.org/10.1098/rspb.2013.3313>.
- Goutte, A., Bustamante, P., Barbraud, C., Delord, K., Weimerskirch, H., Chastel, O., 2014b. Demographic responses to mercury exposure in two closely related antarctic top predators. *Ecology* 95, 1075–1086. <https://doi.org/10.1890/13-1229.1>.
- Gratz, L.E., Keeler, G.J., Blum, J.D., Sherman, L.S., 2010. Isotopic composition and fractionation of mercury in Great Lakes precipitation and ambient air. *Environ. Sci. Technol.* 44, 7764–7770. <https://doi.org/10.1021/es100383w>.
- Heimbürger, L.-E., Sonke, J.E., Cossa, D., Point, D., Lagane, C., Laffont, L., Galfond, B.T., Nicolaus, M., Rabe, B., van der Loeff, M.R., 2015. Shallow methylmercury production in the marginal sea ice zone of the central Arctic Ocean. *Sci. Rep.* 5, 10318. <https://doi.org/10.1038/srep10318>.
- Jiménez-Moreno, M., Perrot, V., Epov, V.N., Monperrus, M., Amouroux, D., 2013. Chemical kinetic isotope fractionation of mercury during abiotic methylation of Hg(II) by methylcobalamin in aqueous chloride media. *Chem. Geol.* 336, 26–36. <https://doi.org/10.1016/j.chemgeo.2012.08.029>.
- Kirk, J., St. Louis, V.L., Hintelmann, H., Lehnher, I., Else, B., Poissant, L., 2008. Methylated mercury species in marine waters of the Canadian High and Sub Arctic. *Env. Sci. Technol.* 42, 8367–8373. <https://doi.org/10.1021/es801635m>.
- Kritee, K., Blum, J.D., Johnson, M.W., Bergquist, B.A., Barkay, T., 2007. Mercury stable isotope fractionation during reduction of Hg(II) to Hg(0) by mercury resistant microorganisms. *Environ. Sci. Technol.* 41, 1889–1895. <https://doi.org/10.1021/es062019t>.
- Kritee, K., Blum, J.D., Barkay, T., 2008. Mercury stable isotope fractionation during reduction of Hg(II) by different microbial pathways. *Environ. Sci. Technol.* 42, 9171–9177. <https://doi.org/10.1021/es801591k>.
- Kritee, K., Barkay, T., Blum, J.D., 2009. Mass dependent stable isotope fractionation of mercury during mer mediated microbial degradation of monomethylmercury. *Geochim. Cosmochim. Acta* 73, 1285–1296. <https://doi.org/10.1016/j.gca.2008.11.038>.
- Kritee, K., Motta, L.C., Blum, J.D., Tsui, M.T.-K., Reinfeld, J.R., 2017. Photomicrobial visible light-induced magnetic mass independent fractionation of mercury in a marine microalga. *ACS Earth Sp. Chem.* 2, 432–440. <https://doi.org/10.1021/acsearthspacechem.7b00056>.
- Kwon, S.Y., Blum, J.D., Carvan, M.J., Basu, N., Head, J.A., Madenjian, C.P., David, S.R., 2012. Absence of fractionation of mercury isotopes during trophic transfer of methylmercury to freshwater fish in captivity. *Environ. Sci. Technol.* 46, 7527–7534. <https://doi.org/10.1021/es300794q>.
- Lamborg, C.H., Hammerschmidt, C.R., Bowman, K.L., Swarr, G.J., Munson, K.M., Ohnemus, D.C., Lam, P.J., Heimbürger, L.-E., Rijkenberg, M.J.A., Saito, M.A., 2014. A global ocean inventory of anthropogenic mercury based on water column measurements. *Nature* 512, 65–68. <https://doi.org/10.1038/nature13563>.
- Lavoie, R.A., Jardine, T.D., Chumchal, M.M., Kidd, K.A., Campbell, L.M., 2013. Biomagnification of mercury in aquatic food webs: a worldwide meta-analysis. *Environ. Sci. Technol.* 47, 13385–13394. <https://doi.org/10.1021/es403103t>.
- Lehnher, I., St. Louis, V.L., Hintelmann, H., Kirk, J.L., 2011. Methylation of inorganic mercury in polar marine waters. *Nat. Geosci.* 4, 298–302. <https://doi.org/10.1038/ngeo1134>.
- Li, M., Sherman, L.S., Blum, J.D., Grandjean, P., Mikkelsen, B., Weihe, P., Sunderland, E.M., Shine, J.P., 2014. Assessing sources of human methylmercury exposure using stable mercury isotopes. *Environ. Sci. Technol.* 48, 8800–8806. <https://doi.org/10.1021/es500340r>.
- Liu, H., Yu, B., Fu, J., Li, Y., Yang, R., Zhang, Q., Liang, Y., Yin, Y., Hu, L., Shi, J., Jiang, G., 2019. Different circulation history of mercury in aquatic biota from King George Island of the Antarctic. *Environ. Pollut.* 250, 892–897. <https://doi.org/10.1016/j.envpol.2019.04.113>.
- Marshall, J., Speer, K., 2012. Closure of the meridional overturning circulation through Southern Ocean upwelling. *Nat. Geosci.* 5, 171–180. <https://doi.org/10.1038/ngeo1391>.
- Masbou, J., Sonke, J.E., Amouroux, D., Guillou, G., Becker, P.R., Point, D., 2018. Hg-stable isotope variations in marine top predators of the Western Arctic Ocean. *ACS Earth Sp. Chem.* 2, 479–490. <https://doi.org/10.1021/acsearthspacechem.8b00017>.
- Mason, R.P., Reinfeld, J.R., Morel, F.M.M., 1996. Uptake, toxicity and trophic transfer of Hg in a coastal diatom. *Environ. Sci. Technol.* 30, 1835–1845. <https://doi.org/10.1021/es950373d>.
- Monperrus, M., Tessier, E., Amouroux, D., Leynaert, A., Huonnic, P., Donard, O.F.X., 2007. Mercury methylation, demethylation and reduction rates in coastal and marine surface waters of the Mediterranean Sea. *Mar. Chem.* 107, 49–63. <https://doi.org/10.1016/j.marchem.2007.01.018>.
- Motta, L.C., Blum, J.D., Johnson, M.W., Umhau, B.P., Popp, B.N., Washburn, S.J., Drazen, J.C., Benitez-Nelson, C.R., Hannides, C.C.S., Close, H.G., Lamborg, C.H., 2019. Mercury cycling in the North Pacific Subtropical Gyre as revealed by mercury stable isotope ratios. *Glob. Biogeochem. Cycles* 33, 777–794. <https://doi.org/10.1029/2018GB006057>.
- Perrot, V., Pastukhov, M.V., Epov, V.N., Husted, S., Donard, O.F.X., Amouroux, D., 2012. Higher mass-independent isotope fractionation of methylmercury in the pelagic food web of Lake Baikal (Russia). *Environ. Sci. Technol.* 46, 5902–5911. <https://doi.org/10.1021/es204572g>.
- Perrot, V., Bridou, R., Pedrero, Z., Guyoneaud, R., Monperrus, M., Amouroux, D., 2015. Identical Hg isotope mass dependent fractionation signature during methylation by sulfate-reducing bacteria in sulfate and sulfate-free environment. *Environ. Sci. Technol.* 49, 1365–1373. <https://doi.org/10.1021/es5033376>.
- Pickhardt, P.C., Folt, C.L., Chen, C.Y., Klaupe, B., Blum, J.D., 2002. Algal blooms reduce the uptake of toxic methylmercury in freshwater food webs. *Proc. Natl. Acad. Sci. U. S. A.* 99, 4419–4423. <https://doi.org/10.1073/pnas.072510999>.
- Point, D., Sonke, J.E., Day, R.D., Roseneau, D.G., Hobson, K.A., Pol, S.S., Vander, Moors, A.J., Pugh, R.S., Donard, O.F.X., Becker, P.R., 2011. Methylmercury photodegradation influenced by sea-ice cover in Arctic marine ecosystems. *Nat. Geosci.* 4, 1–7. <https://doi.org/10.1038/ngeo1049>.
- Queipo Abad, S., Rodríguez-González, P., Davis, W.C., García Alonso, J.L., 2017. Development of a common procedure for the determination of methylmercury, ethylmercury, and inorganic mercury in human whole blood, hair, and urine by triple spike species-specific isotope dilution mass spectrometry. *Anal. Chem.* 89, 6731–6739. <https://doi.org/10.1021/acs.analchem.7b00966>.
- R Core Team, 2016. *R: A Language and Environment for Statistical Computing*. R Foundation for Statistical Computing, Vienna, Austria.
- Renedo, M., Amouroux, D., Pedrero, Z., Bustamante, P., Cherel, Y., 2018a. Identification of sources and bioaccumulation pathways of MeHg in subantarctic penguins: a stable isotopic investigation. *Sci. Rep.* 8, 8865. <https://doi.org/10.1038/s41598-018-27079-9>.
- Renedo, M., Amouroux, D., Duval, B., Carravieri, A., Tessier, E., Barre, J., Bérail, S., Pedrero, Z., Cherel, Y., Bustamante, P., 2018b. Seabird tissues as efficient biomonitoring tools for Hg isotopic investigations: implications of using blood and feathers from chicks and adults. *Environ. Sci. Technol.* 52, 4227–4234. <https://doi.org/10.1021/acs.est.8b00422>.
- Riaux-Gobin, C., Dieckmann, G.S., Poulin, M., Neveux, J., Labrune, C., Vétion, G., 2013. Environmental conditions, particle flux and sympagic microalgal succession in spring before the sea-ice break-up in Adélie Land, East Antarctica. *Polar Res.* 32. <https://doi.org/10.3402/polar.v32i0.19675>.
- Rodrigues, J.L., Rodriguez Alvarez, C., Rodriguez Fariñas, N., Berzas Nevado, J.J., Barbosa, F.J., Rodriguez Martin-Doimeadys, C.R., 2011. Mercury speciation in whole blood by gas chromatography coupled to ICP-MS with a fast microwave-assisted sample preparation procedure. *J. Anal. At. Spectrom.* 26, 436–442. <https://doi.org/10.1039/c004931j>.
- Rodriguez Gonzalez, P., Epov, V.N., Bridou, R., Tessier, E., Guyoneaud, R., Monperrus, M., Amouroux, D., 2009. Species-specific stable isotope fractionation of mercury during Hg (II) methylation by an anaerobic bacteria (*Desulfobulbus propionicus*) under dark conditions. *Environ. Sci. Technol.* 43, 9183–9188. <https://doi.org/10.1021/es902206j>.
- Rose, C.H., Ghosh, S., Blum, J.D., Bergquist, B.A., 2015. Effects of ultraviolet radiation on mercury isotope fractionation during photo-reduction for inorganic and organic mercury species. *Chem. Geol.* 405, 102–111. <https://doi.org/10.1016/j.chemgeo.2015.02.025>.
- Sallée, J.B., Speer, K.G., Rintoul, S.R., 2010. Zonally asymmetric response of the Southern Ocean mixed-layer depth to the Southern. *Nat. Geosci.* 3, 273–279. <https://doi.org/10.1038/ngeo812>.
- Senn, D.B., Chesney, E.J., Blum, J.D., Bank, M.S., Maage, A., Shine, J.P., 2010. Stable isotope (N, C, Hg) study of methylmercury sources and trophic transfer in the Northern Gulf of Mexico. *Environ. Sci. Technol.* 44, 1630–1637. <https://doi.org/10.1021/es902361j>.
- Sherman, L.S., Blum, J.D., Johnson, K.P., Keeler, G.J., Barres, J.A., Douglas, T.A., 2010. Mass-independent fractionation of mercury isotopes in Arctic snow driven by sunlight. *Nat. Geosci.* 3, 173–177. <https://doi.org/10.1038/ngeo758>.
- Sherman, L.S., Blum, J.D., Douglas, T.A., Steffen, A., 2012a. Frost flowers growing in the Arctic ocean-atmosphere-sea ice-snow interface: 2. Mercury exchange between the atmosphere, snow, and frost flowers. *J. Geophys. Res. Atmos.* 117, 1–10. <https://doi.org/10.1029/2011JD016186>.
- Sherman, L.S., Blum, J.D., Keeler, G.J., Demers, J.D., Dvonch, J.T., 2012b. Investigation of local mercury deposition from a coal-fired power plant using mercury isotopes. *Environ. Sci. Technol.* 46, 382–390. <https://doi.org/10.1021/es202793c>.
- Soerensen, A.L., Jacob, D.J., Schartup, A.T., Fisher, J.A., Lehnher, I., St. Louis, V.L., Heimbürger, L.E., Sonke, J.E., Krabbenhoft, D.P., Sunderland, E.M., 2016. A mass budget for mercury and methylmercury in the Arctic Ocean. *Glob. Biogeochem. Cycles* 30, 560–575. <https://doi.org/10.1002/2015GB005280>.
- Sokolov, S., 2008. Chlorophyll blooms in the Antarctic Zone south of Australia and New Zealand in reference to the Antarctic Circumpolar Current fronts and sea ice forcing. *J. Geophys. Res. Ocean.* 113. <https://doi.org/10.1029/2007JC004329>.
- Sokolov, S., Rintoul, S.R., 2007. On the relationship between fronts of the Antarctic Circumpolar Current and surface chlorophyll concentrations in the Southern Ocean. *J. Geophys. Res. Ocean.* 112, 1–17. <https://doi.org/10.1029/2006JC004072>.
- Sullivan, C.W., Arrigo, K.R., McClain, C.R., Comiso, J.C., Firestone, J., 1993. Distributions of phytoplankton blooms in the Southern Ocean. *Science* 262, 1832–1837. <https://doi.org/10.1126/science.262.5141.1832>.
- Sunderland, E.M., Krabbenhoft, D.P., Moreau, J.W., Strode, S.A., Landing, W.M., 2009. Mercury sources, distribution, and bioavailability in the North Pacific Ocean: insights from data and models. *Glob. Biogeochem. Cycles* 23, 1–14. <https://doi.org/10.1029/2008GB003425>.
- Tartu, S., Goutte, A., Bustamante, P., Angelier, F., Moe, B., Clément-Chastel, C., Bech, C., Gabrielsen, G.W., Bustnes, J.O., Chastel, O., 2013. To breed or not to breed: endocrine response to mercury contamination by an Arctic seabird. *Biol. Lett.* 9, 20130317. <https://doi.org/10.1098/rsbl.2013.0317>.
- Tripathy, S.C., Pavithran, S., Sabu, P., Pillai, H.U.K., Dessai, D.R.G., Anilkumar, N., 2015. Deep chlorophyll maximum and primary productivity in Indian Ocean sector of the Southern Ocean: Case study in the subtropical and Polar Front during austral summer 2011. *Deep. Res. Part II Topical Studies in Oceanography* 118, 240–249. <https://doi.org/10.1016/j.dsr2.2015.01.004>.

- Watras, C.J., Back, R.C., Halvorsen, S., Hudson, R.J.M., Morrison, K.A., Wente, S.P., 1998. Bioaccumulation of mercury in pelagic freshwater food webs. *Sci. Total Environ.* 219, 183–208. [https://doi.org/10.1016/S0048-9697\(98\)00228-9](https://doi.org/10.1016/S0048-9697(98)00228-9).
- Yamakawa, A., Takeuchi, A., Shibata, Y., Berail, S., Donard, O.F.X., 2016. Determination of Hg isotopic compositions in certified reference material NIES no. 13 human hair by cold vapor generation multi-collector inductively coupled plasma mass spectrometry. *Accred. Qual. Assur.* 21, 197–202. <https://doi.org/10.1007/s00769-016-1196-x>.
- Zheng, W., Hintelmann, H., 2009. Mercury isotope fractionation during photoreduction in natural water is controlled by its Hg/DOC ratio. *Geochim. Cosmochim. Acta* 73, 6704–6715. <https://doi.org/10.1016/j.gca.2009.08.016>.
- Zheng, W., Hintelmann, H., 2010. Isotope fractionation of mercury during its photochemical reduction by low-molecular-weight organic compounds. *J. Phys. Chem. A* 114, 4246–4253. <https://doi.org/10.1021/jp9111348>.
- Zheng, W., Xie, Z., Bergquist, B.A., 2015. Mercury stable isotopes in ormithogenic deposits as tracers of historical cycling of mercury in Ross Sea, Antarctica. *Env. Sci Technol* 49, 7623–7632. <https://doi.org/10.1021/acs.est.5b00523>.